Applied Energy 353 (2024) 122110

Contents lists available at ScienceDirect

Applied Energy

journal homepage: www.elsevier.com/locate/apenergy

In-situ catalytic upgrading of bio-oils from rapid pyrolysis of torrefied giant miscanthus (*Miscanthus x giganteus*) over copper-magnesium bimetal modified HZSM-5

Virdi Chaerusani [a], Yusrin Ramli [a], Aghietyas Choirun Az Zahra [a], Pan Zhang [b,c], Jenny Rizkiana [d], Suwadee Kongparakul [e], Chanatip Samart [e], Surachai Karnjanakom [f], Dong-Jin Kang [g], Abuliti Abudula [a], Guoqing Guan [a,b,*]

[a] Graduate School of Science and Technology, Hirosaki University, 3-Bunkyocho, Hirosaki 036-8561, Japan
[b] Energy Conversion Engineering Laboratory, Institute of Regional Innovation (IRI), Hirosaki University, 3-Bunkyocho, Hirosaki 036-8561, Japan
[c] Department of Environmental Science and Technology, North China Electric Power University, Baoding, Hebei 071000, China
[d] Department of Chemical Engineering, Institut Teknologi Bandung, Ganesha 10, Bandung 40132, Indonesia
[e] Department of Chemistry, Faculty of Science and Technology, Thammasat University, Pathum Thani 12120, Thailand
[f] Department of Chemistry, Faculty of Science, Rangsit University, Pathum Thani 12000, Thailand
[g] Teaching and Research Center for Bio-coexistence, Faculty of Agriculture and Life Science, Hirosaki University, 84-Ashino, Goshogawara 037-0202, Japan

HIGHLIGHTS

- Fast pyrolysis of both raw and torrefied giant miscanthus (GM) was investigated.
- Phenol and aliphatic hydrocarbons in bio-oil were increased by using torrefied GM.
- In-situ upgrading of raw bio-oils over metal doped zeolites were further studied.
- All spent catalysts were easily regenerated by a simple calcination method.
- Reaction mechanism of the catalytic upgrading process was proposed and discussed.

GRAPHICAL ABSTRACT

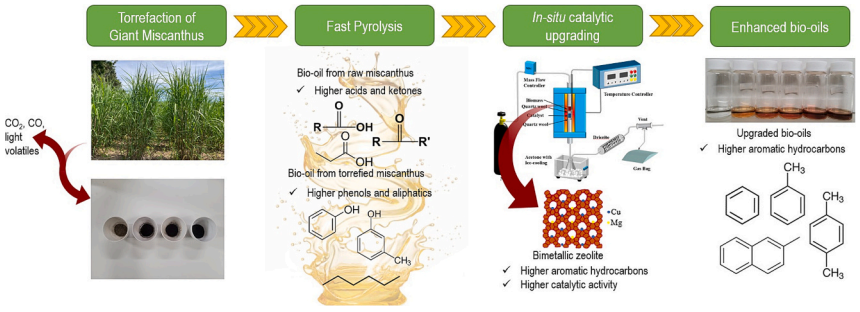

ARTICLE INFO

Keywords:
Torrefaction
Biomass
Bio-oil
Cu-Mg doped HZSM-5
Catalytic upgrading

ABSTRACT

In this study, fast pyrolysis of both raw and torrefied giant miscanthus (GM) is investigated in detail. It is found that the pyrolysis of torrefied GM results in higher distribution of phenols and aliphatic compounds in bio-oil with lower moisture content. To further improve the bio-oil quality, catalytic upgrading process of the bio-oil from the torrefied GM over copper-magnesium (Cu—Mg) bimetal doped zeolites is also investigated. As a result, a highest yield of aromatic hydrocarbons of 63.1% favoring in higher monoaromatic hydrocarbons such as benzene, toluene and xylene in the upgraded bio-oil is obtained as GM-300 is used as feedstock and HSZ-Cu 2:1 Mg as the catalyst. It is found that Cu—Mg doping can not only enhance catalytic activity of zeolite but also maintain relatively low coke deposition and improve the catalyst reusability. Besides, the spent catalysts are

* Corresponding author at: Energy Conversion Engineering Laboratory, Institute of Regional Innovation (IRI), Hirosaki University, 3-Bunkyocho, Hirosaki 036-8561, Japan.
E-mail address: guan@hirosaki-u.ac.jp (G. Guan).

https://doi.org/10.1016/j.apenergy.2023.122110
Received 28 June 2023; Received in revised form 13 September 2023; Accepted 11 October 2023

easily regenerated only by a facile calcination way, and the regenerated catalyst shows almost the same activity as the initial one.

1. Introduction

Nowadays, liquid hydrocarbon-based fuels made from fossil fuels are still the majority of the existing energy infrastructure and account for around 20% of worldwide energy consumption [1–3]. Meanwhile, the demand for various petrochemical products like BTX (benzene, toluene, xylene), and other aromatic hydrocarbons used as fuel or chemical feedstock is still high. Owing to environment issues and diminishing fossil fuel reserves, renewable and sustainable alternatives for making transportation fuel and high value chemicals have been widely explored [4,5].

Biomass is considered as the most promising candidate among those potential renewable energy resources including wind, solar, and hydro powers to reduce overall carbon emission in the future. As the unparalleled renewable carbon-cycling energy source, biomass has many advantages such as sustainability, environment-friendly, and carbon neutrality. In 2015, renewable energy accounted for 19% of total global energy demand, rising by 0.17% each year since 2010 [6], and until now, it is still increasing. With the increase in the demand for renewable energy, besides those traditional biomass resources, biomass energy crops such as Miscanthus are attracting more and more attentions in the world. One of the most common miscanthus species widely grown as an energy crop is giant miscanthus (*Miscanthus x giganteus,* GM) due to its high biomass yield, rapid growth, and relatively easy to grow in various environments without special management [7,8]. Approximately, GM consists of cellulose (45.5%), hemicellulose (29.2%), and lignin (23.8%) [9], which can be transformed into liquid fuel or high value chemicals via a series of chemical conversion routes. Among them, thermochemical conversions such as rapid pyrolysis is one of promising methods for the conversion of biomass to bio-oil with a high yield [10,11]. In general, the obtained bio-oil from fast pyrolysis has dark brown color, high viscosity, weak stability and relatively low heating values (16–19 MJ/kg) with distinctive smoky odor [12]. Raw bio-oil typically consists of various compounds including acids, ketones, aldehydes, phenolics, esters, ethers, furans, sulfur containing compounds and miscellaneous organics, and always has relatively low energy density, limiting its utilization as ideal energy source [13]. Therefore, the raw bio-oil needs to be upgraded prior to use.

Torrefaction is a way for the pre-treatment of biomass to improve the energy density, grindability and storage period, in which biomass is generally heated to a temperature in the range of around 200–300 °C [14,15]. During the torrefaction process, most of the moisture content and some light volatiles are removed. As such, the torrefied biomass will have low moisture content with higher hydrophobicity and better grindability, which should be more convenient to transport and have better resistance to environmental degradation [16,17]. Moreover, the torrefied biomass always shows lower O/C and H/C ratios with improved energy density when compared with the raw biomass.

For the high-quality bio-oil production, besides biomass pretreatment, chemical and physical upgrading methods of raw bio-oil have been studied intensively, in which the most promising way is catalytic upgrading including cracking and deoxygenation reactions at atmospheric pressure, and has gained more attention in recent years [18]. The main target of catalytic upgrading process is to obtain more aromatic hydrocarbons in the final product, which can be either used as high value chemicals or blended with fossil-based fuels to decrease CO_2 emissions during the using. Zeolite has been considered as a more suitable catalyst for this process because of its low cost, high performance, and reusability, which can catalytically convert oxygenated chemicals into aromatic hydrocarbons [19]. Among different types of zeolites, HZSM-5 is considered the most promising one because of its narrow pore diameter and shape selectivity for converting oxygenated compounds into aromatic hydrocarbons [20,21].

To further improve the catalytic activity of zeolites, many researchers modified zeolite structures by incorporating metals such as Cu, Ni, Fe, Mo, Sn, Mg, etc. The metal doped zeolite could have new active sites with enhanced catalytic activity. Widayatno et al. [22] reported that the incorporation of low-content Cu species (0.25–3 wt%) on zeolite could improve catalyst acidity and enhance the activity as well as aromatic hydrocarbons selectivity. However, higher acidity of zeolite could enhance secondary cracking and polymerization of volatiles into coke, which will inversely decrease the catalyst activity and stability to produce aromatic hydrocarbons. To overcome these disadvantages, combining Cu with alkali earth metals with basic properties has been found to have great potential to further improve the aromatic hydrocarbons yield by adjusting the textural properties and acidities of zeolite [23]. Nowadays, only several studies on the bimetal-doped zeolites that combine both acidic and basic properties of the metals to improve selectivity, stability, and reusability have been reported.

In this study, various Cu—Mg doped zeolites with both acid and base characteristics were synthesized for upgrading of bio-oils from the rapid pyrolysis of raw and torrefied GM. The product compositions in the bio-oils originating from raw and torrefied GMs were measured at first. Then, the best sample resulting in bio-oil with the best quality was further investigated in the catalytic upgrading using both monometal- and bimetal-doped zeolites to understand the effect of metal doping on the product selectivity and quality. Moreover, the catalyst reusability was examined for 3 cycles in the cases with and without regeneration. As we known, no researchers reported such zeolite-based catalysts so far and thus, it is expected to widely apply them in the upgrading of bio-oil as well as the production of high value-added chemical feedstock especially aromatic hydrocarbons from biomass.

2. Experimental

2.1. Biomass preparation

Giant miscanthus (GM) was collected in autumn from Aomori, Japan, which was cracked into particles with a size of 1–3 mm and oven-dried at 110 °C for 24 h. A tube reactor was used to produce torrefied GMs, in which N_2 gas with a flow rate of 100 cm^3/min was used to create an inert atmosphere inside the reactor. The bulk raw biomass was fed to the reactor and torrefied with a residence time of 60 min. The torrefactions were performed at 200, 250, and 300 °C, respectively with a heating rate of 20 °C/min and the obtained samples are named as GM-200, GM-250 and GM-300, respectively. Finally, both raw and torrefied GM samples were cracked to a particle size of 0.5–1 mm and stored at a vacuum sealed box.

2.2. Catalyst preparation

The commercial zeolite (HZSM-5 Zeolite, Si/Al = 40) was purchased from TOSOH Corp. Before using, the zeolite powder was calcined in air for 4 h at 650 °C to move out those adsorbed impurities. The pretreated zeolite was doped with Cu and Mg species by a wet impregnation route. In brief, 25 mL of distilled water was used to dissolve a specified amount of $Cu(NO_3)_2.3H_2O$, which then constantly agitated to produce a clear blue color solution. A given quantity of $Mg(NO_3)_2.3H_2O$ was also introduced to the above solution with stirring. After both salts were completely dissolved, a given amount of zeolite was introduced into it to obtain a slurry, which was continuously stirred for 6 h with a magnetic stirrer. The obtained slurry was heated in an oven at 110 °C overnight

before being calcined at 550 °C for around 4 h. By this method, Cu—Mg bimetal doped zeolites with Cu:Mg molar ratios of 1:0, 1:1, 2:1, 1:2, 0:1 were obtained and named as HSZ—Cu, HSZ-Cu 1:1 Mg, HSZ-Cu 2:1 Mg, HSZ-Cu 1:2 Mg and HSZ—Mg, respectively. The details on the characterizations of biomass and catalysts are described in the Supplementary Materials.

The experiment on the biomass pyrolysis with a fixed bed reactor, the process for catalytic upgrading of bio-oils, and the characterizations of obtained bio-oils are further explained in the Supplementary Materials.

3. Results and discussion

3.1. Characterization of biomass

SEM images of the biomass (Fig. S2) before and after torrefaction were observed for a better understanding of the impact on morphology of the biomass during the torrefaction. Obviously, the surface of GM is flat and relatively smooth while for the torrefied biomass obtained at a higher torrefaction temperature has a significantly different microstructure when compared to the raw biomass. During the torrefaction, especially under the temperature of 300 °C for 1 h, the cell-wall disintegration and a relatively rough structure are visible, and microapertures are created owing to the damages in the torrefaction process. This could be attributed to the devolatilization and carbonization under the torrefaction condition with the removal of epidermis layer [24]. As shown in Fig. S2, the surface morphologies of GM and torrefied GM are associated with the devolatilization intensity during the torrefaction.

The proximate and ultimate analysis results of GM and torrefied GM are presented in Table 1. After the torrefaction, both fixed carbon and ash content increase, and torrefaction at 300 °C reduces the volatile content of GM to 31.12% from 69.66% due to the devolatilization of light organic compounds [25]. With a higher torrefaction temperature, the oxygen and hydrogen contents also decrease. Consequently, the HHV of torrefied GM is increased after the torrefaction. Whereas, both H/C and O/C ratios of the torrefied GM decrease with the increase in the torrefaction temperature, suggesting that major reactions could be dehydration and deoxygenation during the torrefaction process.

Figs. 1 and 2 show thermogravimetric (TG) and derivative thermogravimetric (DTG) analysis results for GM and torrefied GM, respectively. One can see that thermal decomposition process can be separated into three stages. The first stage occurred before 200 °C should be related to moisture vaporization and light volatile matters removal from the biomass. In the second stage, a sudden weight decrease occurs between 200 and 400 °C owing to the depolymerization of both hemicellulose and cellulose in GM. In the third stage, a slow mass decrease after the temperature of 400 °C is found, which could be attributed to the degradation of lignin inside GM [24,26]. Obviously, the first stage is more dominant for the raw GM and still visible for GM-200 sample. In comparison, for GM-300 sample, the first stage becomes not so obvious because most of the moisture content and light volatile have been removed after the torrefaction. The second stage of mass loss is due to the degradation of hemicellulose and cellulose. Higher loss of mass is visible for raw GM at this stage and the mass loss gradually decreases along with samples prepared at a higher torrefaction temperature. Generally, the degradation temperature of hemicellulose is the lowest (200–300 °C), cellulose starts to degrade at the temperature of around 300–400 °C and lignin will decompose at a wide temperature range (200–900 °C) [27]. As can be seen in DTG profiles, the raw GM and GM-200 mainly exhibit 2 mass loss peaks, representing the moving of remained water and the decomposition/evaporation of light volatiles while the second peak represents the overlapped depolymerizations of hemicellulose, cellulose, and lignin. The torrefied GM obtained at higher torrefaction temperature results in a lower peak of moisture and almost no peak of moisture detected after being torrefied at a temperature of 300 °C, indicating that almost all the moisture was removed from raw GM during the high temperature torrefaction process (refer to Table 1). In most cases, mass loss of hemicellulose creates a shoulder peak in DTG profiles at the temperature range of around 200–300 °C. In this work, for

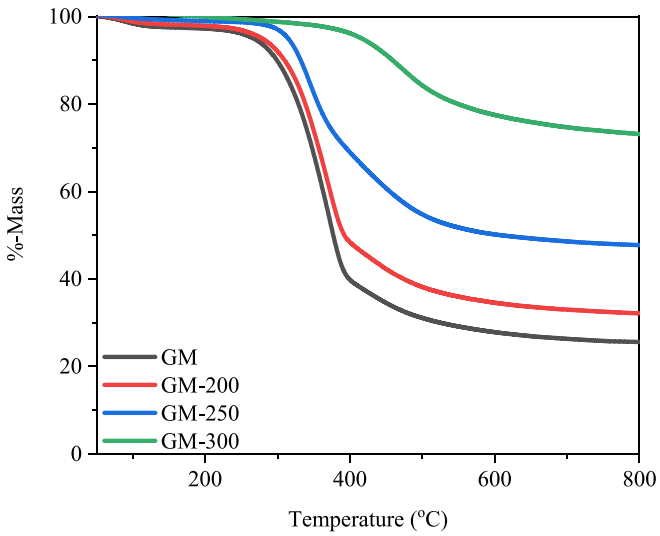

Fig. 1. Thermogravimetric analyses of raw and torrefied biomass feedstocks.

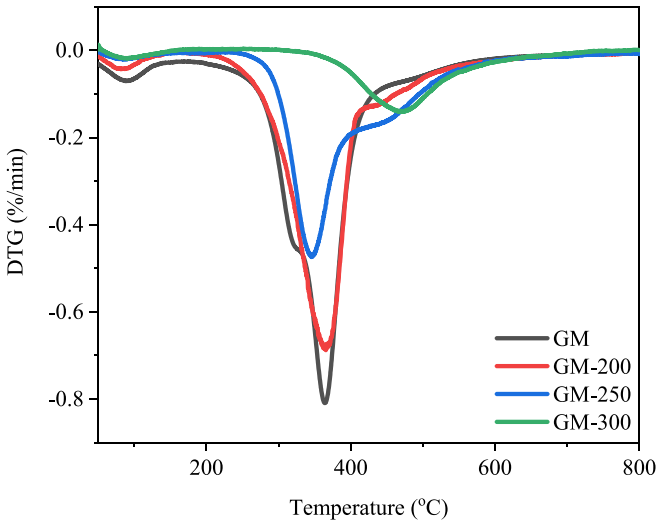

Fig. 2. DTG profiles of raw and torrefied biomass feedstocks.

Table 1
Proximate and ultimate analysis results of raw and torrefied GM samples.

	GM	GM-200	GM-250	GM-300
Proximate analysis (wt%)				
Moisture	5.58	1.62	1.09	0.43
Volatile	69.66	63.52	51.41	31.12
Fixed Carbon	24.76	23.58	32.68	44.63
Ash	8.72	11.28	14.82	23.82
Ultimate analysis (wt%)				
C	42.56	47.11	52.37	58.38
H	5.85	4.91	4.66	2.96
O	50.02	45.36	40.30	36.11
N	1.57	2.62	2.67	2.55
S	0.00	0.00	0.00	0.00
H/C	0.13	0.10	0.08	0.05
O/C	1.17	0.96	0.76	0.61
HHV	16.37	17.26	19.25	19.59

the torrefied GM sample, the shoulder peak is difficult to distinguish and looks like that it is overlapped with the peaks relating to cellulose and lignin decompositions. This result could be due to the relatively lower content of hemicellulose in the torrefied GM sample [28]. The decomposition rate also decreases significantly after 400 °C owing to the slow decomposition rate of lignin and secondary cracking of carbonaceous compounds. It is also worth mentioning that the obvious mass loss point of torrefied GM is shifted to the higher temperature range when a higher temperature is applied for preparing the torrefied GM since the decomposition of hemicellulose as well as cellulose will be more severe [29,30].

Fig. 3 displays XRD profiles of raw and torrefied GM samples. The higher degree of torrefaction results in the gradual decrease in the peak intensity at $2\theta = 22°$, and at the same time, some peaks at $2\theta = 24°$, 28°, 41°, 51°, 66°, 58°, and 74° are observed, which correspond to the crystalline structure of potassium chloride, indicating that K and Cl species exist in the GM. The FTIR spectra of raw and torrefied GM under different temperatures are displayed in Fig. 4, in which the peaks at 1090, 1641, 2920 and 3290 cm^{-1} are observed. These peaks are attributed to the C—O bonds in lignin, stretching of C═O in cellulose, stretching vibration of C—H bond in cellulose, and stretching vibration of O—H from moisture content inside the biomass. With a higher degree of torrefaction, the OH functional group peak intensity becomes weaker, which confirms the dehydration phenomenon in the torrefaction process [31].

3.2. Characterizations of catalysts

XRD diffraction peaks of parent HZSM-5 and various metal doped zeolites were examined. As displayed in Fig. 5, all metal doped zeolites still retain the crystalline structure of parent one after the metal doping, indicating that Cu and Mg doping does not change crystal structure of the parent zeolite. It is worth mentioning that the peaks corresponding to Cu and Mg are not found for the doped samples, implying that both Cu and Mg species should be well dispersed on the parent zeolite, which could effectively reduce the agglomeration of copper and magnesium species on zeolite surface during the reaction.

Fig. 6 shows NH_3-TPD spectra of both parent and metal doped HZSM-5 zeolites. Obviously, there are two desorption peaks at low and high temperature ranges, which are relating to the weaker acid sites (Lewis acid) and stronger acid sites (Brønsted acid) on the catalysts, consecutively. One can see that the intensity of desorption peaks on weak acid sites increases after Cu doping since some of the H^+ on the catalyst are ion-exchanged by Cu^{2+}. Whereas, after the Mg doping, the acidity of

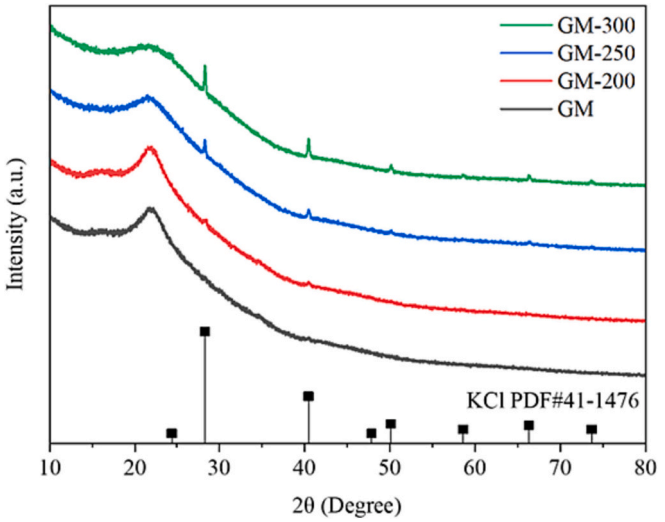

Fig. 3. XRD patterns of raw and torrefied biomass feedstocks.

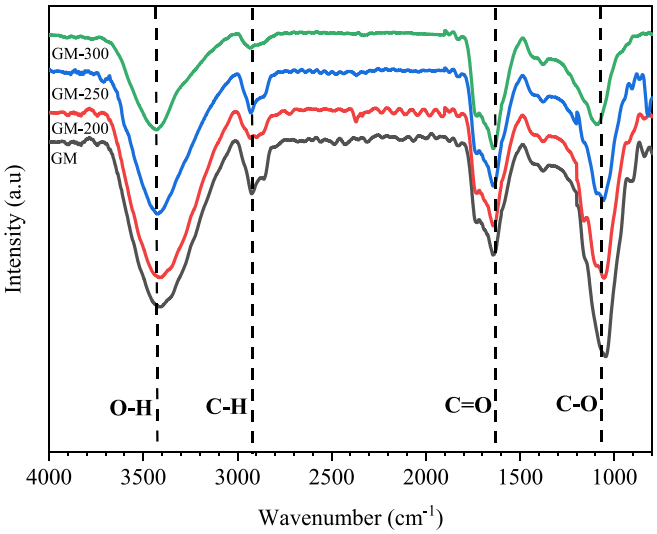

Fig. 4. FTIR spectra of raw and torrefied biomass feedstocks.

parent HZSM-5 zeolite drops since the magnesium species has more basic characteristics. Herein, after metal doping, various metals (Me) species including Me-O-Si and Me-O could co-exist and conveniently interact on the active sites of zeolite, resulting in the reorganization of zeolite structure and formation of a new framework among dislocated Si and Al species [32].

Fig. 7 shows pore size distributions of the prepared zeolite catalyst samples. Obviously, all the catalysts present a narrow pore size distribution with a range of 2–10 nm. The specific surface areas, pore volumes, and pore sizes are listed in Table 2. For the metal doped HZSM-5 catalysts, the pore size, pore volume and surface area are significantly reduced since both copper and magnesium species could deposit in the internal and external pores of zeolites and change the surface properties. In general, larger molecules could easily get in those larger pores and reach the inside active sites of pores. Notedly, coke could be generated in the pores more easily owing to the polycondensation, leading to catalyst deactivation [33]. Therefore, it is necessary to fabricate optimum pore structure in order to enhance catalysis stability in the catalytic upgrading process of bio-oil.

FTIR spectra of both parent and Cu—Mg doped HZSM-5 zeolites are depicted in Fig. 8. The observed frequencies at 570, 800, 1100, 1635, 3450 and 3620 cm^{-1} are in a good agreement with the data of the literature [34,35]. Herein, the broad peak at 3450–3700 cm^{-1} is associated with the Si-OH and Si(*OH*)Al framework structure, which can contribute Brønsted acid sites. The broad peak in the range of 3100–3550 cm^{-1} is related to the OH stretching on the extra framework of aluminum species, and the band intensity after Cu—Mg doping is slightly lower compared to the parent catalyst. This might be due to a decrease in O—H bond strength after metal incorporation to the zeolite framework [36].

Fig. S3 shows the surface morphology and EDX mappings of the metal doped HZSM-5 zeolites. It is found that no bulk copper or magnesium species are formed on the zeolite surface. Here, a well distribution of metal species on the zeolite surface is also ensured via EDX analysis, which is in accordance with the XRD analysis results. However, it should be noted that the metal doped zeolite tends to agglomerate due to the linkage of smaller HZSM-5 crystals [37].

3.3. Product distributions after torrefaction treatment

The chemical compositions of bio-oil derived from the pyrolysis of GM and torrefied GM are shown in Fig. 9. Here, the bio-oil components can be classified into 7 groups, i.e., aromatic hydrocarbons, ketones, phenols, aliphatic hydrocarbons, aldehydes, acidic compound, and

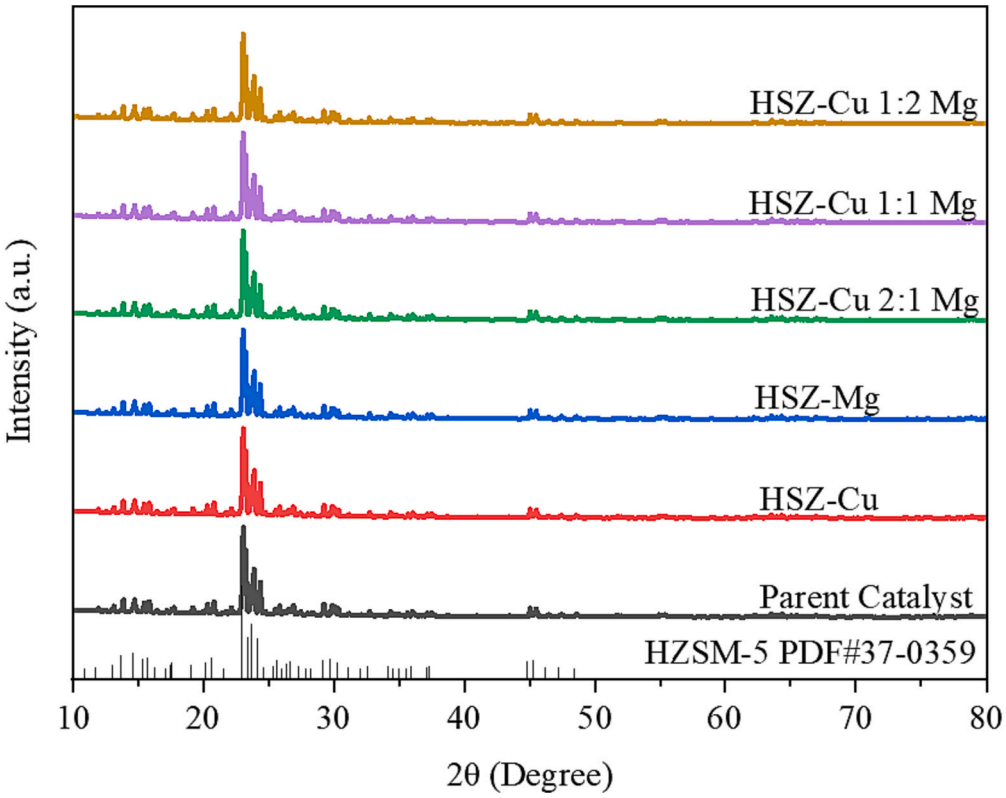

Fig. 5. XRD patterns of parent and metal doped zeolites.

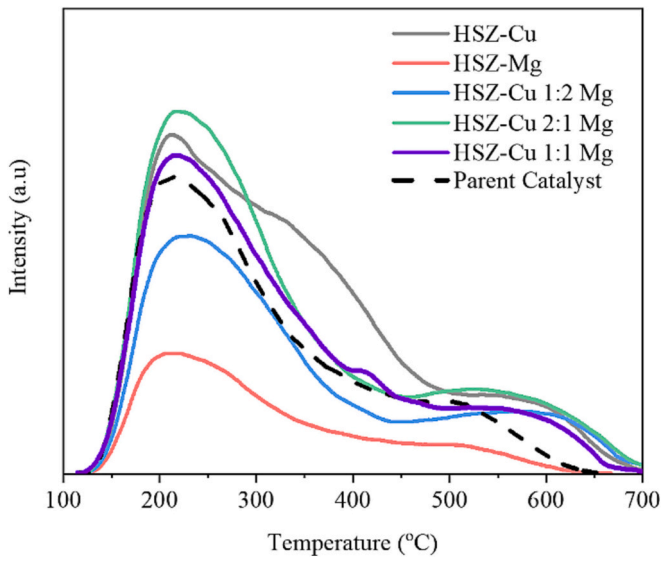

Fig. 6. NH_3-TPD profiles of the parent and metal doped zeolites used in this study.

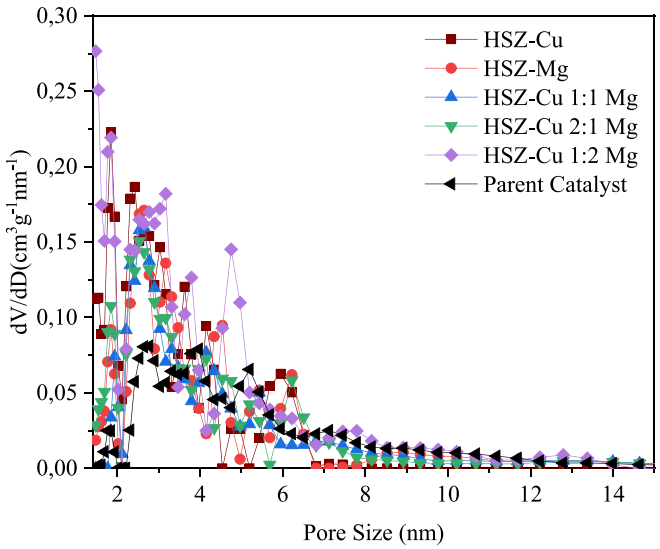

Fig. 7. Pore size distributions of the parent and metal doped zeolites used in this study.

others. The bio-oil generated from the raw GM mostly contains oxygenates such as acid and ketones, accounting for 65.58%. The high oxygenates amount should be attributed to the higher oxygen percentage and lower carbon percentage in raw GM. For the bio-oil derived from the torrefied GM, the product distributions are changed, especially the concentration of acids and ketones are reduced. It is reported that these oxygenates are mainly derived from the depolymerization, dehydration and cracking of cellulose and hemicellulose [38]. As such, for the torrefied GM, hemicellulose and cellulose have been decomposed to some extent, which will affect the pyrolysis result. On the other hand, more phenols and aliphatic compounds in the bio-oil from the torrefied GM are generated and the increased extent is enhanced for the torrefied GM obtained at a higher torrefaction temperature. The depolymerization of hemicellulose and cellulose always occurs during the torrefaction, making the components relating to lignin become the main constituent in the torrefied biomass, which is the precursor of phenols in the pyrolysis bio-oil. While, aliphatic hydrocarbons are mostly produced from the reorganization of radicals generated by deoxygenation and ring opening of cellulose and the splitting of alkyl linkages of lignin [39]. Therefore, higher lignin content in the torrefied GM should be benefit

Table 2
Acidities and textural properties of the parent and metal doped HZSM-5 zeolites.

Catalyst	Acidities			Textural Properties		
	Lewis Acid sites (mmol/g, low temp.)	Brønsted Acid Sites (mmol/g, high temp.)	Total Acidity (mmol/g)	S_{BET} (m^2/g)	V_{total} (cm^3/g)	Average pore size (nm)
HSZ-Cu	0.631	0.194	0.825	370.06	0.21	2.35
HSZ-Mg	0.256	0.052	0.308	245.85	0.25	2.70
HSZ-Cu 1:2 Mg	0.388	0.224	0.612	231.79	0.22	2.85
HSZ-Cu 1:1 Mg	0.555	0.207	0.762	280.14	0.20	2.40
HSZ-Cu 2:1 Mg	0.683	0.212	0.895	261.12	0.31	2.56
Parent Catalyst	0.527	0.174	0.711	332.66	0.20	2.44

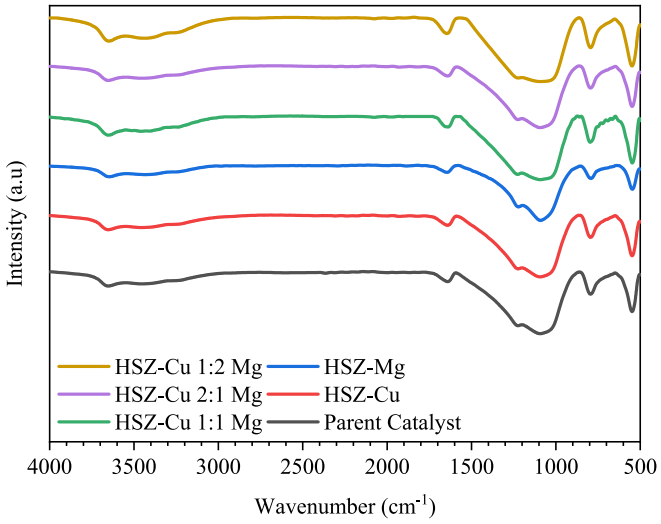

Fig. 8. FTIR spectra of parent and metal doped zeolites used in this study.

for the generation of aliphatic hydrocarbons during the fast pyrolysis.

Pyrolysis products generally have 4 groups, oil, gas, water, and char as shown in Fig. 10. Pyrolysis of torrefied biomass prepared at a higher torrefaction temperature from 200 to 300 °C leads to a higher char yield from 25.4% to 38.1% but significantly lower water yield from 28.6% to 10.8%. As stated above, during the torrefaction process, thermal devolatilization and carbonization will occur, which will change the torrefied GM decomposition pathway during further pyrolysis, thereby enhancing char formation and reducing volatilization [40]. In addition, torrefaction at a higher temperature will lead to the formation of thermally stable structures, preventing the generation of volatiles during further pyrolysis [41]. The corresponding gas product distributions are shown in Fig. 11. Obviously, total gas yield from the pyrolysis of torrefied GM is lower than that from the raw GM, especially carbon dioxide and carbon monoxide. As stated above, during the torrefaction, both hemicellulose and cellulose will be partially depolymerized, leading to lower formation of carbon oxide gases during the further pyrolysis [42]. Based on these results, GM-300 was chosen as the best substrate to be further investigated in the catalytic upgrading process.

3.4. Product distribution in the catalytic upgrading of torrefied GM

The performances of metal doped HZSM-5 zeolites for the catalytic upgrading of bio-oils obtained from the rapid pyrolysis of GM-300 were tested in a fixed bed reactor and the bio-oils was analyzed with GC–MS instrument. Here, the components in the bio-oils can be classified into 7 groups, i.e., aromatic hydrocarbons, ketones, phenols, aliphatic hydrocarbons, aldehydes, acidic compound, and others. Among these compounds, aromatic hydrocarbon is selected as the indicator to evaluate the catalytic performance. As shown in Fig. 12, with the presence of parent catalyst, the total relative quantity of aromatic hydrocarbons is 48.6%. Metal doping on the parent HZSM-5 zeolite further improves the

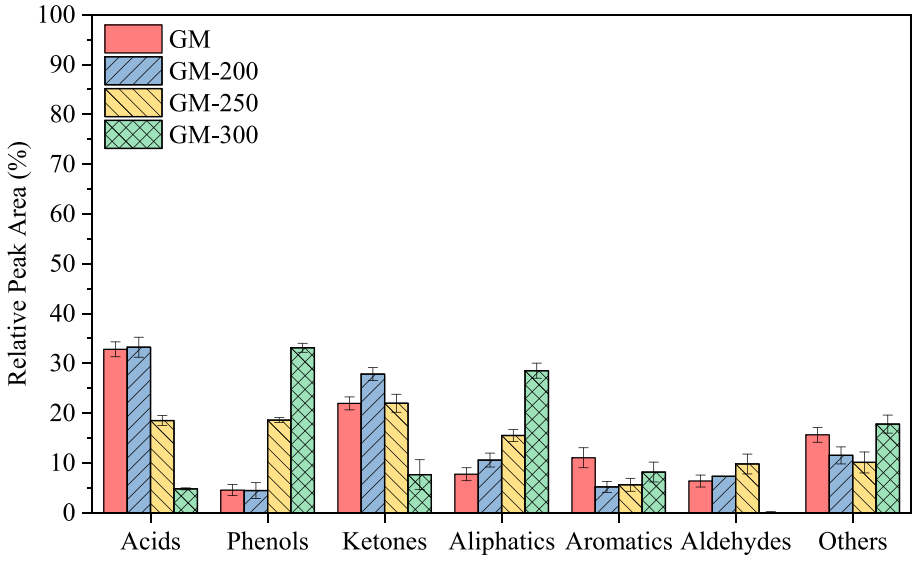

Fig. 9. Chemical compositions of bio-oils derived from fast pyrolysis of raw and torrefied biomass.

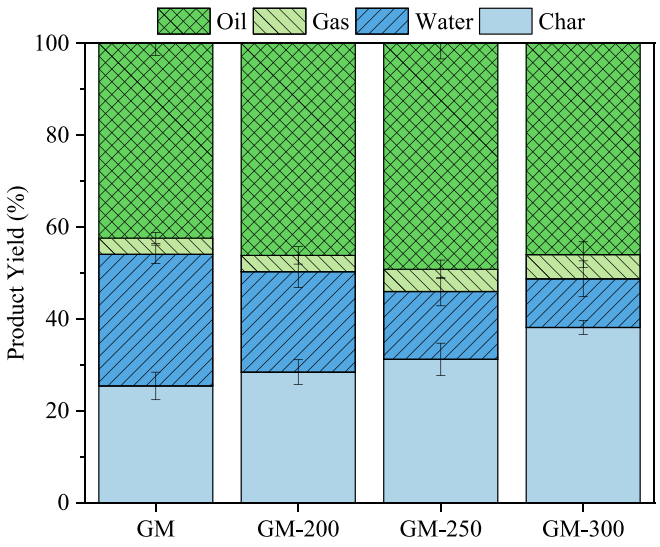

Fig. 10. Product distributions of bio-oils derived from fast pyrolysis of raw and torrefied biomass.

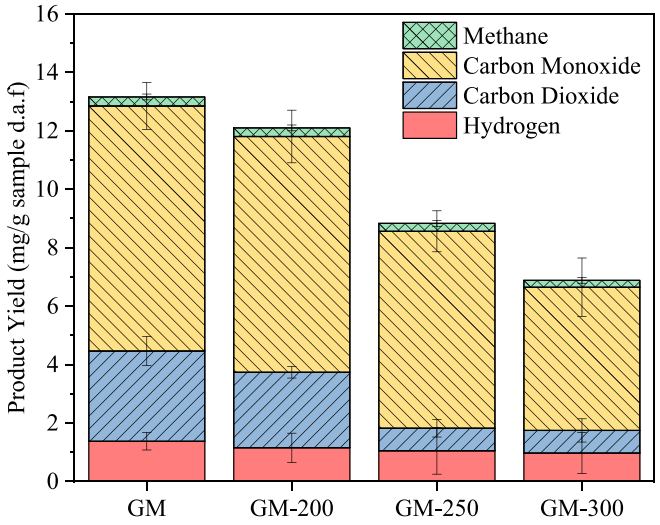

Fig. 11. Gas yields during fast pyrolysis of raw and torrefied biomass.

aromatic hydrocarbons yield with a highest relative amount of 63.1%. The higher selectivity toward aromatic hydrocarbons and the lower selectivity toward phenols indicate that metal doping can improve the conversion of phenolic compounds to aromatic hydrocarbons through demethoxylation and dehydroxylation reactions [43]. Other oxygenated compounds such as ketones are also reduced significantly using the metal doped HZSM-5 zeolites. The deoxygenation pathway of ketones and phenol is generally carried out via three pathways, i.e., decarbonylation, dehydration, and decarboxylation [44]. Compared with the monometal doped HZSM-5 zeolites and parent HZSM-5 zeolite, the Cu—Mg bimetal doped HZSM-5 zeolites possess higher relative yields of aromatic hydrocarbons. It should be due to the incorporation of Cu and Mg species and the synergistic effect of the two active sites, which can improve the deoxygenation pathways toward aromatic hydrocarbons. Thus, the addition of Cu and Mg species on the zeolite support could further enhance the removal of oxygenated compounds in bio-oil.

In this study, the identified aromatic hydrocarbons are toluene, benzene, p-xylene, o-xylene, ethylbenzenes including monoaromatic hydrocarbons (MAHs), naphtalene and indene as polyaromatic hydrocarbons (PAHs). As we can see in Fig. 13, in the cases using HSZ-Cu and HSZ-Mg catalysts, relative quantity of aromatic hydrocarbons content in the upgraded bio-oil is increased to 51.7% and 50.6%. Interestingly, in the case using Cu-doped catalyst, naphtalene and indene (PAHs) yields increase while toluene (MAHs) yield decreases significantly. In contrast, in the case using Mg-doped catalyst, benzene, toluene and xylene (MAHs) yields increase while the production of naphtalene and indene (PAHs) is hindered. This might be related to the enhanced hydrogen transfer ability and the optimized acid properties of the catalysts by the metal modification [45]. Furthermore, the minimum PAHs yield of 1.6% is obtained by using the HSZ-Cu 1:2 Mg catalyst, which is about 75% lower than that by using HSZ-Parent. These results indicate that Mg doping could prevent some of the PAHs formation during the catalytic upgrading process. In addition, the increased coke production on the catalyst surface could be a result of increased PAHs generation during upgrading process. Thereby, it is always expected to lower PAHs yield in order to inhibit the coke generation and prolong the life-time of catalyst activity [46].

Fig. 14 shows the percentages of detected products during in-situ catalytic upgrading process of bio-oil with parent and metal doped HZSM-5 zeolites. Herein, the products are divided into 5 groups, i.e., oil, water, char, gas, and coke deposited on catalyst surface after the upgrading process. It is found that after metal doping on zeolite catalyst, lower coke is formed on most of them when compared to that on the parent catalyst. However, for the HSZ—Cu, slightly higher coke is deposited on its surface, leading to the lowest oil yield. This could be due to the enhanced strong acid sites after Cu doping, which could enhance either deoxygenation process or some secondary reactions such as polycondensation, cyclization, and polymerization of primary products including aromatic hydrocarbons, phenols, ketones to generate coke on catalyst surface, leading to a lower oil yield with higher coke deposition [47]. It is also observed that the lowest coking extent is achieved by using HSZ-Mg catalyst with a 6.6% yield. Mg doping on zeolite could provide some basicity in the catalyst to prevent some of the secondary polymerization of hydrocarbons. These could be benefit for catalyst reusability due to lower coke formation on catalyst surface [48]. In addition, more water is generated when the parent zeolite is doped with both Cu and Mg. These findings suggest that several reactions related to the production of light gases and water including dehydrogenation, dehydration, decarbonylation, decarboxylation, and cracking are responsible for the formation of hydrocarbons, gases, coke, and water. Therefore, the incorporating of Cu and Mg in zeolites is of great significance to form acid-base bifunctional characteristics. Such a bifunctional catalyst system could give some advantages during catalytic upgrading to improve aromatic hydrocarbons yield, maintain relatively low water content in bio-oil and reduce coke deposition on catalyst surface, thereby maintaining the catalytic activity of zeolites and improving product quality. For the gas yield, as shown in Fig. S4, the use of parent catalyst results in lower gas product than those using the metal doped zeolites. The increase of gas yield, especially CO_2 and CO, in the cases using metal doped zeolites should be related to dehydrogenation, dehydration, decarbonylation, and decarboxylation, along with the formation of aromatic hydrocarbons and the reduction of oxygenated compounds in the upgraded bio-oils [49,50]. More CO_2 and CO, especially CO, are produced when metal doped zeolites are utilized. It suggested that decarbonylation could be the major reaction during the bio-oil deoxygenation.

3.5. Reaction mechanism during bio-oil upgrading with bimetal doped catalysts

According to the above analyses and considering the main three compounds of hemicellulose, cellulose and lignin in both raw and torrefied GMs, the possible reaction pathways in the in-situ catalytic upgrading of bio-oils over bimetal doped zeolite catalysts are summarized in Fig. 15. Here, the biomass pyrolysis routes have great relationship with the cellulose, hemicellulose, and lignin components. These

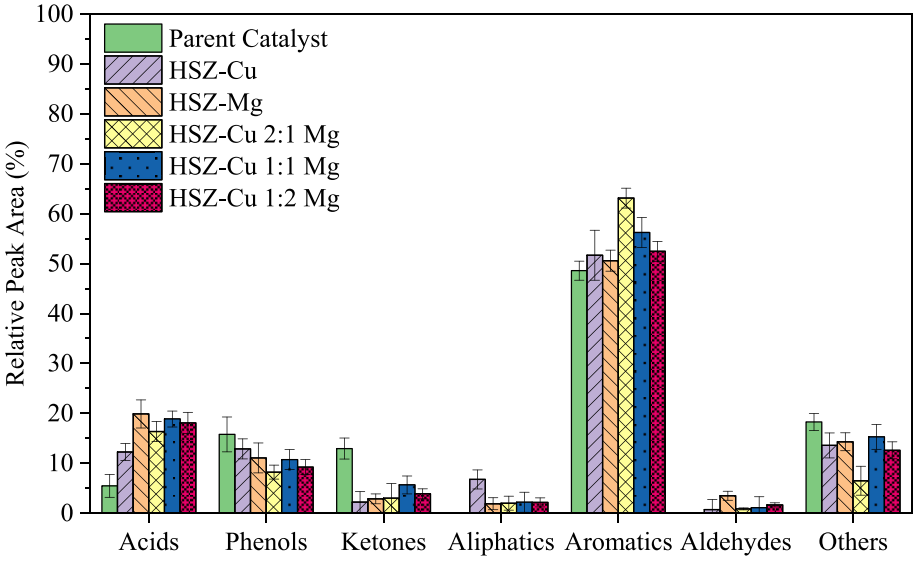

Fig. 12. Chemical compositions of upgraded bio-oils derived from fast pyrolysis of GM-300 with different zeolite catalysts.

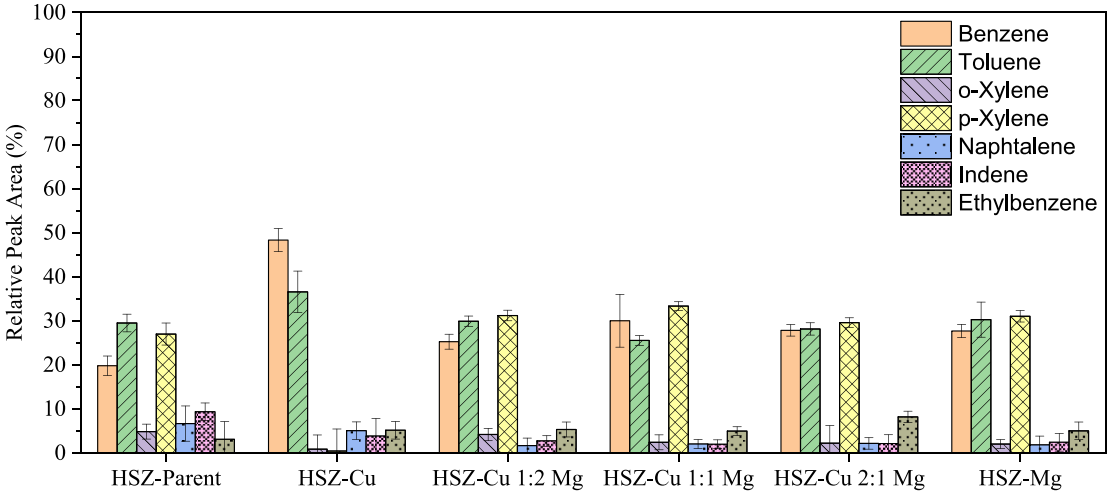

Fig. 13. Aromatic hydrocarbon compositions of upgraded bio-oils derived from fast pyrolysis of GM-300 with different zeolite catalysts.

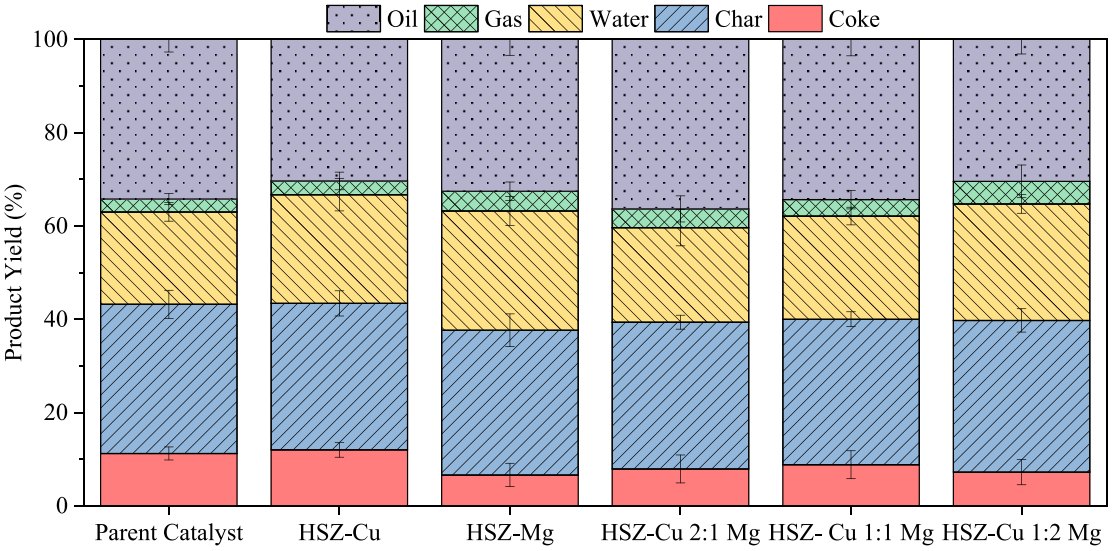

Fig. 14. Product distributions of bio-oils derived from fast pyrolysis of GM-300 with different zeolite catalysts.

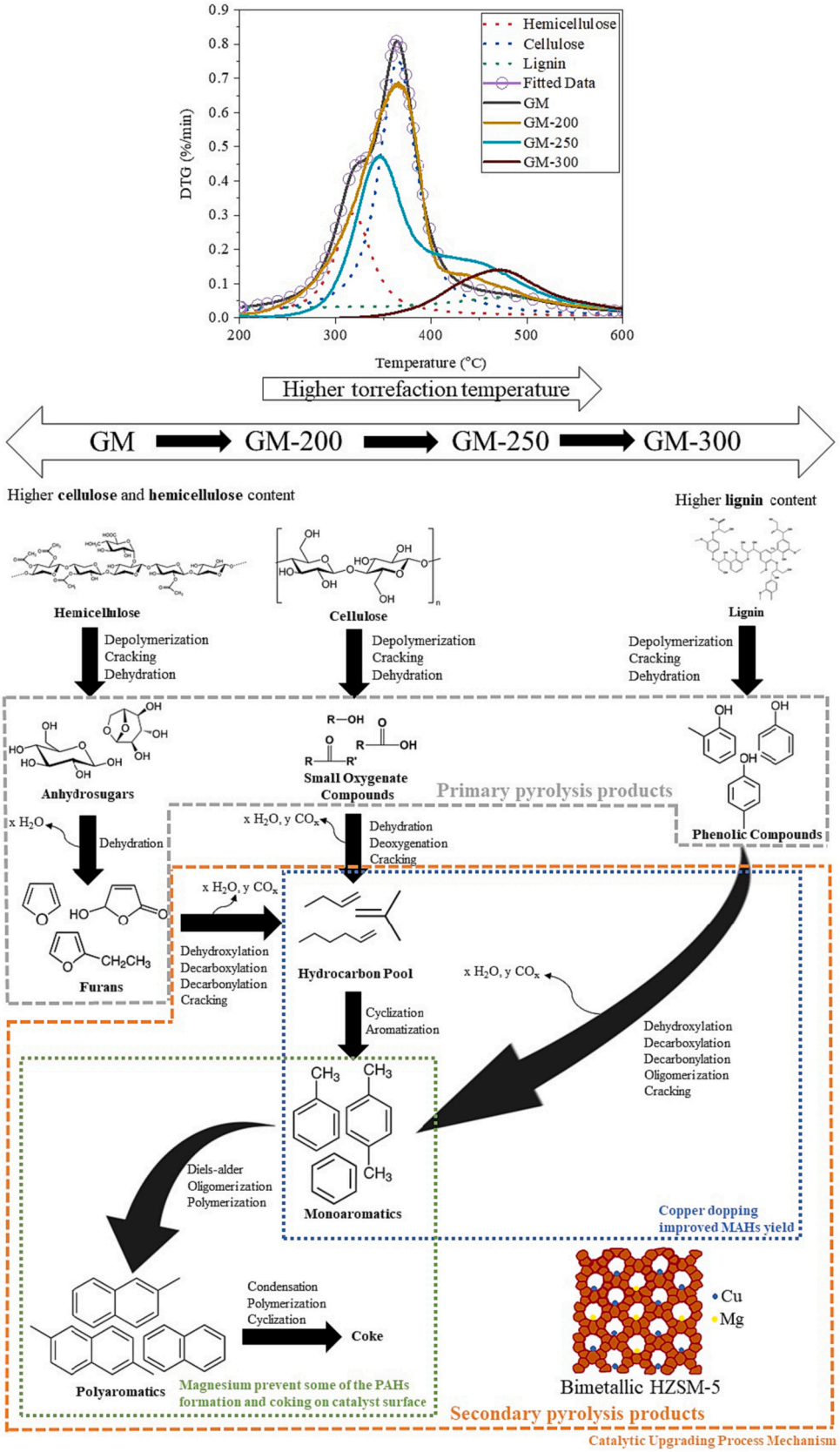

Fig. 15. Possible reaction pathways for aromatic hydrocarbons formation from the catalytic upgrading of bio-oil derived from fast pyrolysis of raw and torrefied GM.

biomass constituents will decompose into smaller oxygenated compounds by different routes under the influence of heat rate during the first pyrolysis step [51]. For example, hemicellulose will undergo a thermal decomposition to form anhydrosugars (e.g., levoglucosan and D-glucose), pyrans, and furans through depolymerization and thermal cracking [52]. Cellulose will thermally decompose into smaller oxygenated compounds (e.g., alcohols, ketones, aldehydes), and depolymerization of lignin will form phenolic compounds. It should be noted that torrefaction of raw GM will change the percentages of various biomass constituents (hemicellulose, cellulose and lignin). During the torrefaction, raw GM undergoes carbonization and devolatilization, leading to an increase of lignin content with the loss of cellulose and hemicellulose.

The lower percentage of cellulose and hemicellulose can be ascribed to chemical degradation after the torrefaction process [53]. This will shift the reaction pathway and the primary pyrolysis products toward lignin derived constituents in the pyrolysis of torrefied GM. That is, those primary pyrolysis products could be upgraded in the secondary pyrolysis step, in which some oxygenated compounds could be more easily diffuse into the zeolite micropores and transform into aromatic hydrocarbons. During the catalytic upgrading process, zeolite parameters play some important roles. For example, pore size of zeolite will determine whether the primary pyrolysis products could diffuse and enter the acid sites. Large molecules such as alkoxyl phenols could combine on the surface of zeolite and undergo polymerization to form coke under the influence of strong external acid sites. For the conversion of the primary pyrolysis products into aromatic hydrocarbons, the appropriate number of acid sites plays an important role [54]. In this study, doping the zeolite with Cu and Mg could balance the total acid sites in zeolite to obtain optimum aromatic hydrocarbons yield and maintain relatively low coke deposition on the zeolite surface. Additionally, the pore size would be altered after metal doping on zeolite, which would partially replace the Brønsted acid into Lewis acid sites [55]. Another reason is the accelerated hydrogen migration between acid sites and metals, drastically improving the conversion of oxygenated compounds into MAHs. The deoxygenation pathway can be shifted to decarbonylation reactions as evidenced by the increase of carbon oxide gases. As stated above, Cu doping adds more acidities on zeolite, which can promote secondary cracking of the pyrolysis vapor into carbon oxide gases. However, Mg doping increases carbon monoxide yield significantly with the decrease of coke yield, suggesting that Mg doping may be able to reduce the production of coke through the stimulation of atomic hydrogen movement via activation of C—H on the active sites. The possible reaction mechanism for coke removal from catalyst surface in the presence of Mg is proposed as follows [56,57]:

$$Mg_2O - C + H_2O \rightarrow Mg_2O_2 - C + H_2 \quad (1)$$

$$x\ Mg_2O_2 - C + x\ C \rightarrow x\ Mg_2O - C + x\ CO \quad (2)$$

$$(1-x)\ Mg_2O_2 - C + (1-x)\ CO \rightarrow (1-x)\ Mg_2O - C + (1-x)\ CO_2 \quad (3)$$

$$\text{Overall}: x\ C + H_2O \rightarrow H_2 + (2x-1)\ CO + (1-x)\ CO_2 \quad (4)$$

It is also found that the use of Cu—Mg doped zeolites not only favours deoxygenation reaction, but also promotes the oligomerization, Diels-Alder, alkylation, and aromatization reactions to produce higher aromatic hydrocarbons yield and maintain a relatively low coke yield.

3.6. Reusability of catalysts

The reusability of metal doped zeolite and parent zeolite catalysts was examined at a suitable temperature of 500 °C and using GM-300 as the biomass feedstock for the catalytic upgrading. Fig. 16 summarizes the results in the reusing of catalyst for 3 cycles and the regenerated catalyst. One can see that HSZ-Cu 2:1 Mg exhibits high selectivity and stability with only a minor decrease of aromatic hydrocarbons yield after each cycle, where the decrease is no more than 10% compared to the first cycle using the fresh catalyst. Parent catalyst exhibits a high reduction in the relative amounts of aromatic hydrocarbons. This reduction of aromatic hydrocarbon yield could be attributed to coking on catalyst surface after several cycles, leading to catalyst deactivation. Higher coke deposition was observed on the parent catalyst without metal doping than that on the metal doped catalyst. Interestingly, a higher rate of coke deposition on parent catalyst is observed with the increase of cycle. This should be the reason why the parent catalyst exhibits a high reduction of aromatic hydrocarbons yield compared to the metal doped catalysts used in this work. Herein, Cu and Mg doping serves as additional active sites that can improve aromatic hydrocarbons yield during catalytic upgrading process. Higher acidity resulting from Cu doping can improve MAHs formation while Mg doping prevents some of the secondary polymerization with the coking resistance on catalyst surface during the upgrading process. As a result, using both metals simultaneously improves aromatic hydrocarbons yield and maintains relatively low coke deposition on active sites of the catalyst. After using for the 3rd cycle, each of the spent catalyst was regenerated via a facile calcination process in air at 550 °C for 3 h. It is found that the regenerated catalysts exhibit almost the same performances as the initial ones, suggesting that their catalytic activities have been recovered completely.

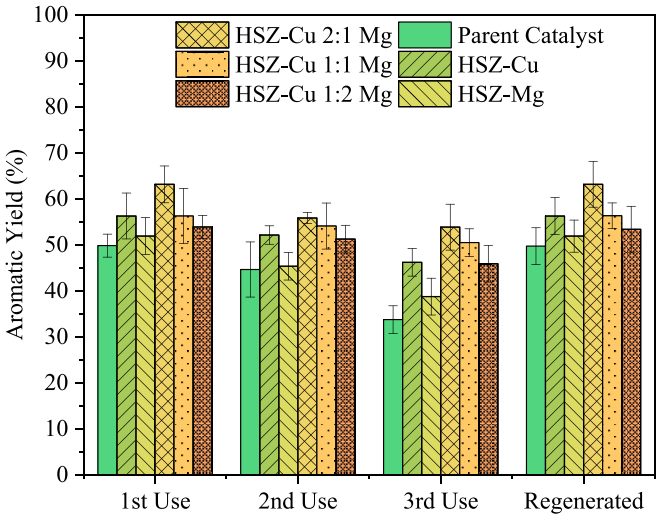

Fig. 16. Aromatic hydrocarbon yields using zeolite catalysts for several times without regeneration and after the regeneration.

4. Conclusions

Pre-treatment of raw GM by torrefaction led to the decomposition of hemicellulose and cellulose, leaving mostly lignin inside the torrefied GM. These resulted in higher aliphatic and phenol compound yields with improved bio-oil quality. The best biomass sample, which is the torrefied GM prepared at 300 °C, was chosen as the feedstock for catalytic upgrading. Catalyst characterization showed that metal species can be dispersed well on the catalyst surface and HSZ-Cu 2:1 Mg demonstrated the highest performance in the generation of aromatic hydrocarbons in the upgraded bio-oils with a high relative percentage of 63.1%. Moreover, the deactivated Cu-Mg-doped zeolites due to coking were successfully recovered by a facile calcination method.

CRediT authorship contribution statement

Virdi Chaerusani: Writing – original draft, Validation, Methodology, Investigation, Formal analysis, Data curation. **Yusrin Ramli:** Investigation. **Aghietyas Choirun Az Zahra:** Investigation. **Pan Zhang:**

Investigation. **Jenny Rizkiana:** Validation. **Suwadee Kongparakul:** Validation. **Chanatip Samart:** Validation. **Surachai Karnjanakom:** Investigation. **Dong-Jin Kang:** Validation, Investigation. **Abuliti Abudula:** Validation, Investigation. **Guoqing Guan:** Writing – review & editing, Validation, Software, Project administration, Methodology, Investigation, Funding acquisition, Conceptualization.

Declaration of Competing Interest

The authors declare that they have no known competing financial interests or personal relationships that could have appeared to influence the work reported in this paper.

Data availability

Data will be made available on request.

Acknowledgements

This work is supported by JST Grant Number JPMJPF2104, Japan, Takahashi Industrial and Economic Research Foundation and Hirosaki University, Japan. The authors acknowledge the Shared Facility Center for Science and Technology, Hirosaki University (SFCST) for SEM and XRD analysis. V. Chaerusani, Y. Ramli, and A. Az Zahra gratefully acknowledge the scholarship from the Ministry of Education, Culture, Sport, Science and Technology (MEXT) of Japan, and P. Zhang gratefully acknowledges the State Scholarship Fund of China Scholarship Council, China.

Appendix A. Supplementary data

Supplementary data to this article can be found online at https://doi.org/10.1016/j.apenergy.2023.122110.

References

[1] Shi Y, Xing E, Wu K, Wang J, Yang M, Wu Y. Recent progress on upgrading of bio-oil to hydrocarbons over metal/zeolite bifunctional catalysts. Cat Sci Technol 2017; 7:2385–415. https://doi.org/10.1039/c7cy00574a.

[2] Altan A, Karasu S. Crude oil time series prediction model based on LSTM network with chaotic Henry gas solubility optimization. Energy 2022;242:122964. https://doi.org/10.1016/j.energy.2021.122964.

[3] Karasu S, Altan A, Bekiros S, Ahmad W. A new forecasting model with wrapper-based feature selection approach using multi-objective optimization technique for chaotic crude oil time series. Energy 2020;212:118750. https://doi.org/10.1016/j.energy.2020.118750.

[4] da Silva CMS, Carneiro ACO, Vital BR, Figueiró CG, Fialho LF, de Magalhães MA, et al. Biomass torrefaction for energy purposes – definitions and an overview of challenges and opportunities in Brazil. Renew Sustain Energy Rev 2018;82: 2426–32. https://doi.org/10.1016/j.rser.2017.08.095.

[5] Zheng Y, Li D, Pei T, Wang J, Liu C, Lu Y, et al. Mechanism of synergistic effects and kinetic analysis in bamboo-LDPE waste ex-situ catalytic co-pyrolysis for enhanced aromatic hydrocarbon production via CeZrAl and HZSM-5 dual catalyst. J Environ Chem Eng 2022;10:0–2. https://doi.org/10.1016/j.jece.2022.107479.

[6] Gielen D, Boshell F, Saygin D, Bazilian MD, Wagner N, Gorini R. The role of renewable energy in the global energy transformation. Energ Strat Rev 2019;24: 38–50. https://doi.org/10.1016/j.esr.2019.01.006.

[7] Xue G, Kwapinska M, Kwapinski W, Czajka KM, Kennedy J, Leahy JJ. Impact of torrefaction on properties of Miscanthus × giganteus relevant to gasification. Fuel 2014;121:189–97. https://doi.org/10.1016/j.fuel.2013.12.022.

[8] Angelini LG, Ceccarini L, Nassi Di Nasso N, Bonari E. Comparison of Arundo donax L. and Miscanthus x giganteus in a long-term field experiment in Central Italy: analysis of productive characteristics and energy balance. Biomass Bioenergy 2009; 33:635–43. https://doi.org/10.1016/j.biombioe.2008.10.005.

[9] Kallis KX, Pellegrini Susini GA, Oakey JE. A comparison between Miscanthus and bioethanol waste pellets and their performance in a downdraft gasifier. Appl Energy 2013;101:333–40. https://doi.org/10.1016/j.apenergy.2012.01.037.

[10] Chen H, Cheng H, Zhou F, Chen K, Qiao K, Lu X, et al. Catalytic fast pyrolysis of rice straw to aromatic compounds over hierarchical HZSM-5 produced by alkali treatment and metal-modification. J Anal Appl Pyrolysis 2018;131:76–84. https://doi.org/10.1016/j.jaap.2018.02.009.

[11] Lehto J, Oasmaa A, Solantausta Y, Kytö M, Chiaramonti D. Review of fuel oil quality and combustion of fast pyrolysis bio-oils from lignocellulosic biomass. Appl Energy 2014;116:178–90. https://doi.org/10.1016/j.apenergy.2013.11.040.

[12] Shahbeik H, Shafizadeh A, Gupta VK, Lam SS, Rastegari H, Peng W, et al. Using nanocatalysts to upgrade pyrolysis bio-oil: a critical review. J Clean Prod 2023; 413:137473. https://doi.org/10.1016/j.jclepro.2023.137473.

[13] Richa L, Colin B, Pétrissans A, Wallace C, Hulette A, Quirino RL, et al. Catalytic and char-promoting effects of potassium on lignocellulosic biomass torrefaction and pyrolysis. Environ Technol Innov 2023;31:103193. https://doi.org/10.1016/j.eti.2023.103193.

[14] Chaluvadi S, Ujjwal A, Singh RK. Effect of Torrefaction prior to biomass size reduction on ethanol production. Waste Biomass Valoriz 2019;10:3567–77. https://doi.org/10.1007/s12649-018-0389-4.

[15] Zhang C, Ho SH, Chen WH, Fu Y, Chang JS, Bi X. Oxidative torrefaction of biomass nutshells: evaluations of energy efficiency as well as biochar transportation and storage. Appl Energy 2019;235:428–41. https://doi.org/10.1016/j.apenergy.2018.10.090.

[16] Nunes LJR, Matias JCO, Catalão JPS. A review on torrefied biomass pellets as a sustainable alternative to coal in power generation. Renew Sustain Energy Rev 2014;40:153–60. https://doi.org/10.1016/j.rser.2014.07.181.

[17] Mehdi R, Raza N, Naqvi SR, Khoja AH, Mehran MT, Farooq M, et al. A comparative assessment of solid fuel pellets production from torrefied agro-residues and their blends. J Anal Appl Pyrolysis 2021;156:105125. https://doi.org/10.1016/j.jaap.2021.105125.

[18] Louwes AC, Basile L, Yukananto R, Bhagwandas JC, Bramer EA, Brem G. Torrefied biomass as feed for fast pyrolysis: an experimental study and chain analysis. Biomass Bioenergy 2017;105:116–26. https://doi.org/10.1016/j.biombioe.2017.06.009.

[19] Mehdi MS, Mehran MT, Naqvi SR, Zaman SU, Khoja AH, Bahadar A. Catalytic pyrolysis of polyethylene waste with Fuller's earth clay and metal oxides under mild conditions. Mater Today Proc 2022;57:1322–8. https://doi.org/10.1016/j.matpr.2021.12.552.

[20] Kurnia I, Karnjanakom S, Bayu A, Yoshida A, Rizkiana J, Prakoso T, et al. In-situ catalytic upgrading of bio-oil derived from fast pyrolysis of lignin over high aluminum zeolites. Fuel Process Technol 2017;167:730–7. https://doi.org/10.1016/j.fuproc.2017.08.026.

[21] Chaihad N, Situmorang YA, Anniwaer A, Kurnia I, Karnjanakom S, Kasai Y, et al. Preparation of various hierarchical HZSM-5 based catalysts for in-situ fast upgrading of bio-oil. Renew Energy 2021;169:283–92. https://doi.org/10.1016/j.renene.2021.01.013.

[22] Widayatno WB, Guan G, Rizkiana J, Yang J, Hao X, Tsutsumi A, et al. Upgrading of bio-oil from biomass pyrolysis over cu-modified β-zeolite catalyst with high selectivity and stability. Appl Catal Environ 2016;186:166–72. https://doi.org/10.1016/j.apcatb.2016.01.006.

[23] Chaerusani V, Zahra ACA, Anniwaer A, Zhang P, Chaihad N, Rizkiana J, et al. Catalytic upgrading of bio-oils derived from terrestrial and marine biomass over various types of zeolites. J Anal Appl Pyrolysis 2022;168:105735. https://doi.org/10.1016/j.jaap.2022.105735.

[24] Xu H, Cheng S, Hungwe D, Yoshikawa K, Takahashi F. Co-pyrolysis coupled with torrefaction enhances hydrocarbons production from rice straw and oil sludge: the effect of torrefaction on co-pyrolysis synergistic behaviors. Appl Energy 2022;327: 120104. https://doi.org/10.1016/j.apenergy.2022.120104.

[25] Lin B, Huang Q, Chi Y. Co-pyrolysis of oily sludge and rice husk for improving pyrolysis oil quality. Fuel Process Technol 2018;177:275–82. https://doi.org/10.1016/j.fuproc.2018.05.002.

[26] Zhang C, Yang W, Chen WH, Ho SH, Pétrissans A, Pétrissans M. Effect of torrefaction on the structure and reactivity of rice straw as well as life cycle assessment of torrefaction process. Energy 2022:240. https://doi.org/10.1016/j.energy.2021.122470.

[27] Zhang Y, Gao Y, Zhao M, Feng X, Wang L, Yang H, et al. Effects of torrefaction on the lignin of apricot shells and its catalytic conversion to aromatics. ACS Omega 2021;6:25742–8. https://doi.org/10.1021/acsomega.1c04095.

[28] Chen WH, Kuo PC. Torrefaction and co-torrefaction characterization of hemicellulose, cellulose and lignin as well as torrefaction of some basic constituents in biomass. Energy 2011;36:803–11. https://doi.org/10.1016/j.energy.2010.12.036.

[29] Wilk M, Magdziarz A. Hydrothermal carbonization, torrefaction and slow pyrolysis of Miscanthus giganteus. Energy 2017;140:1292–304. https://doi.org/10.1016/j.energy.2017.03.031.

[30] Barzegar R, Yozgatligil A, Olgun H, Atimtay AT. TGA and kinetic study of different torrefaction conditions of wood biomass under air and oxy-fuel combustion atmospheres. J Energy Inst 2020;93:889–98. https://doi.org/10.1016/j.joei.2019.08.001.

[31] Chen YC, Chen WH, Lin BJ, Chang JS, Ong HC. Impact of torrefaction on the composition, structure and reactivity of a microalga residue. Appl Energy 2016; 181:110–9. https://doi.org/10.1016/j.apenergy.2016.07.130.

[32] Tshabalala TE, Scurrell MS. Aromatization of n-hexane over Ga, Mo and Zn modified H-ZSM-5 zeolite catalysts. Cat Com 2015;72:49–52. https://doi.org/10.1016/j.catcom.2015.06.022.

[33] Chaihad N, Karnjanakom S, Abudula A, Guan G. Zeolite-based cracking catalysts for bio-oil upgrading: a critical review. Resour Chem Mater 2022. https://doi.org/10.1016/j.recm.2022.03.002.

[34] Nibou D, Amokrane S, Mekatel H, Lebaili N. Elaboration and characterization of solid materials of types zeolite NaA and faujasite NaY exchanged by zinc metallic ions Zn2 +. Phys Proc 2009;2:1433–40. https://doi.org/10.1016/j.phpro.2009.11.113.

[35] Aloulou H, Bouhamed H, Ghorbel A, Ben Amar R, Khemakhem S. Elaboration and characterization of ceramic microfiltration membranes from natural zeolite:

application to the treatment of cuttlefish effluents. Desalin Water Treat 2017;95:9–17. https://doi.org/10.5004/dwt.2017.21348.
[36] Yang F, Zhong J, Liu X, Zhu X. A novel catalytic alkylation process of syngas with benzene over the cerium modified platinum supported on HZSM-5 zeolite. Appl Energy 2018;226:22–30. https://doi.org/10.1016/j.apenergy.2018.05.093.
[37] Ren X, Cao J, Zhao X, Yang Z, Liu S, Wei X. Enhancement of aromatic products from catalytic fast pyrolysis of lignite over hierarchical HZSM-5 by piperidine-assisted desilication enhancement of aromatic products from catalytic fast pyrolysis of lignite over hierarchical HZSM-5 by piperidine-assiste. 2017. https://doi.org/10.1021/acssuschemeng.7b03185.
[38] Dai L, Wang Y, Liu Y, Ruan R, He C, Yu Z, et al. Integrated process of lignocellulosic biomass torrefaction and pyrolysis for upgrading bio-oil production: a state-of-the-art review. Renew Sustain Energy Rev 2019;107:20–36. https://doi.org/10.1016/j.rser.2019.02.015.
[39] Tang CY, Zhang DX. Mechanisms of aliphatic hydrocarbon formation during co-pyrolysis of coal and cotton stalk. Chin Chem Lett 2016;27:1607–11. https://doi.org/10.1016/j.cclet.2016.03.037.
[40] Yu J, Ramirez Reina T, Paterson N, Millan M. On the primary pyrolysis products of torrefied oak at extremely high heating rates in a wire mesh reactor. Appl Energy Combust Sci 2022;9:100046. https://doi.org/10.1016/j.jaecs.2021.100046.
[41] Zheng A, Zhao Z, Chang S, Huang Z, Wang X, He F, et al. Effect of torrefaction on structure and fast pyrolysis behavior of corncobs. Bioresour Technol 2013;128:370–7. https://doi.org/10.1016/j.biortech.2012.10.067.
[42] Chaihad N, Anniwaer A, Karnjanakom S, Kasai Y, Kongparakul S, Samart C, et al. In-situ catalytic upgrading of bio-oil derived from fast pyrolysis of sunflower stalk to aromatic hydrocarbons over bifunctional cu-loaded HZSM-5. J Anal Appl Pyrolysis 2021;155:105079. https://doi.org/10.1016/j.jaap.2021.105079.
[43] Luo Z, Lu K, Yang Y, Li S, Li G. Catalytic fast pyrolysis of lignin to produce aromatic hydrocarbons: optimal conditions and reaction mechanism. RSC Adv 2019;9:31960–8. https://doi.org/10.1039/c9ra02538c.
[44] Kumar R, Strezov V, Kan T, Weldekidan H, He J, Jahan S. Investigating the effect of mono- and bimetallic/zeolite catalysts on hydrocarbon production during bio-oil upgrading from ex situ pyrolysis of biomass. Energy Fuel 2020;34:389–400. https://doi.org/10.1021/acs.energyfuels.9b02724.
[45] Li K, Zhang G, Wang Z, Xiang Hu B, Lu Q. Calcium formate assisted catalytic pyrolysis of pine for enhanced production of monocyclic aromatic hydrocarbons over bimetal-modified HZSM-5. Bioresour Technol 2020;315:123805. https://doi.org/10.1016/j.biortech.2020.123805.
[46] Wu J, Chang G, Li X, Li J, Guo Q. Effects of NaOH on the catalytic pyrolysis of lignin/HZSM-5 to prepare aromatic hydrocarbons. J Anal Appl Pyrolysis 2020;146:104775. https://doi.org/10.1016/j.jaap.2020.104775.
[47] Palizdar A, Sadrameli SM. Catalytic upgrading of biomass pyrolysis oil over tailored hierarchical MFI zeolite: effect of porosity enhancement and porosity-acidity interaction on deoxygenation reactions. Renew Energy 2020;148:674–88. https://doi.org/10.1016/j.renene.2019.10.155.
[48] Karnjanakom S, Guan G, Asep B, Du X, Hao X, Yang J, et al. A green method to increase yield and quality of bio-oil: ultrasonic pretreatment of biomass and catalytic upgrading of bio-oil over metal (Cu, Fe and/or Zn)/γ-Al2O3. RSC Adv 2015;5:83494–503. https://doi.org/10.1039/c5ra14609g.
[49] Karnjanakom S, Guan G, Asep B, Hao X, Kongparakul S, Samart C, et al. Catalytic upgrading of bio-oil over Cu/MCM-41 and Cu/KIT-6 prepared by β-Cyclodextrin-assisted coimpregnation method. J Phys Chem C 2016;120:3396–407. https://doi.org/10.1021/acs.jpcc.5b11840.
[50] Karnjanakom S, Guan G, Asep B, Du X, Hao X, Samart C, et al. Catalytic steam reforming of tar derived from steam gasification of sunflower stalk over ethylene glycol assisting prepared Ni/MCM-41. Energ Conver Manage 2015;98:359–68. https://doi.org/10.1016/j.enconman.2015.04.007.
[51] Zhang Y, Liang Y, Li S, Yuan Y, Zhang D, Wu Y, et al. A review of biomass pyrolysis gas: forming mechanisms, influencing parameters, and product application upgrades. Fuel 2023;347:128461. https://doi.org/10.1016/j.fuel.2023.128461.
[52] Shen D, Zhao J, Xiao R. Catalytic transformation of lignin to aromatic hydrocarbons over solid-acid catalyst: effect of lignin sources and catalyst species. Energ Conver Manage 2016;124:61–72. https://doi.org/10.1016/j.enconman.2016.06.067.
[53] Xue G, Kwapinska M, Horvat A, Kwapinski W, Rabou LPLM, Dooley S, et al. Gasification of torrefied Miscanthus×giganteus in an air-blown bubbling fluidized bed gasifier. Bioresour Technol 2014;159:397–403. https://doi.org/10.1016/j.biortech.2014.02.094.
[54] Karnjanakom S, Bayu A, Hao X, Kongparakul S, Samart C, Abudula A, et al. Selectively catalytic upgrading of bio-oil to aromatic hydrocarbons over Zn, Ce or Ni-doped mesoporous rod-like alumina catalysts. J Mol Catal A Chem 2016;421:235–44. https://doi.org/10.1016/j.molcata.2016.06.001.
[55] Yang G, Zhou L, Han X. Lewis and Brönsted acidic sites in M 4+−doped zeolites (M = Ti, Zr, Ge, Sn, Pb) as well as interactions with probe molecules: a DFT study. J Mol Catal A Chem 2012;363–364:371–9. https://doi.org/10.1016/j.molcata.2012.07.013.
[56] McKee DW. Mechanisms of catalyzed gasification of carbon. 2008. p. 236–55. https://doi.org/10.1063/1.32942.
[57] Karnjanakom S, Suriya-umporn T, Bayu A, Kongparakul S, Samart C, Fushimi C, et al. High selectivity and stability of Mg-doped Al-MCM-41 for in-situ catalytic upgrading fast pyrolysis bio-oil. Energ Conver Manage 2017;142:272–85. https://doi.org/10.1016/j.enconman.2017.03.049.